ATF / ATF2 extraction beam phase space

Philip Bambade

on behalf of:

D.Angal-Kalinin, R.Appleby, J.Jones, T.Scarfe (CI, UK)
M.Alabau (IFIC/LAL), A. Faus-Golfe (IFIC)
G.White (SLAC/LAL), M.Woodley (SLAC), S.Kuroda (KEK)
P.B., J.Brossard, G. Le Meur, Y.Rénier, C.Rimbault, F.Touze (LAL)

6th ATF2 project meeting @ Nanobeam 2008
May 26-30 May, 2008, BINP, Novosibirsk, Russia

ATF2 LAYOUT

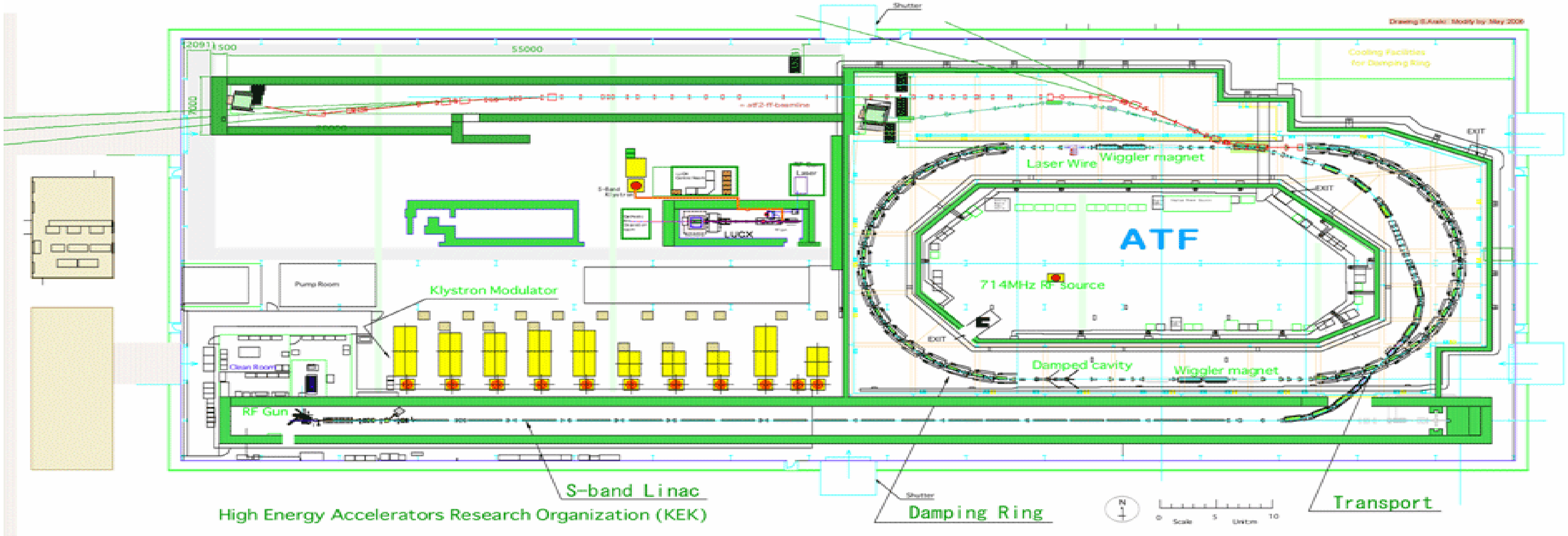

- ATF2 input match stability
- Evidences for emittance growth and reliability
- Phase-space measurements
- Is there a main suspect ?
- Improved automation and collaborative procedures
- Improved instrumentation

ATF EXT line description & wire scanner position

Nominal geometric emittance : ε_x=2nm.rad & ε_y=20 pm.rad

5 positions for wire scanners

Each position is equipped with 3 wire scanners oriented at 0, 90 and 80° for y,x and 10° beam-size measurement.

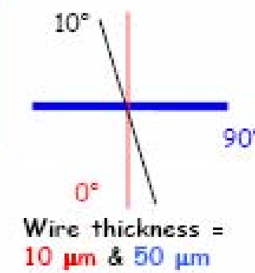

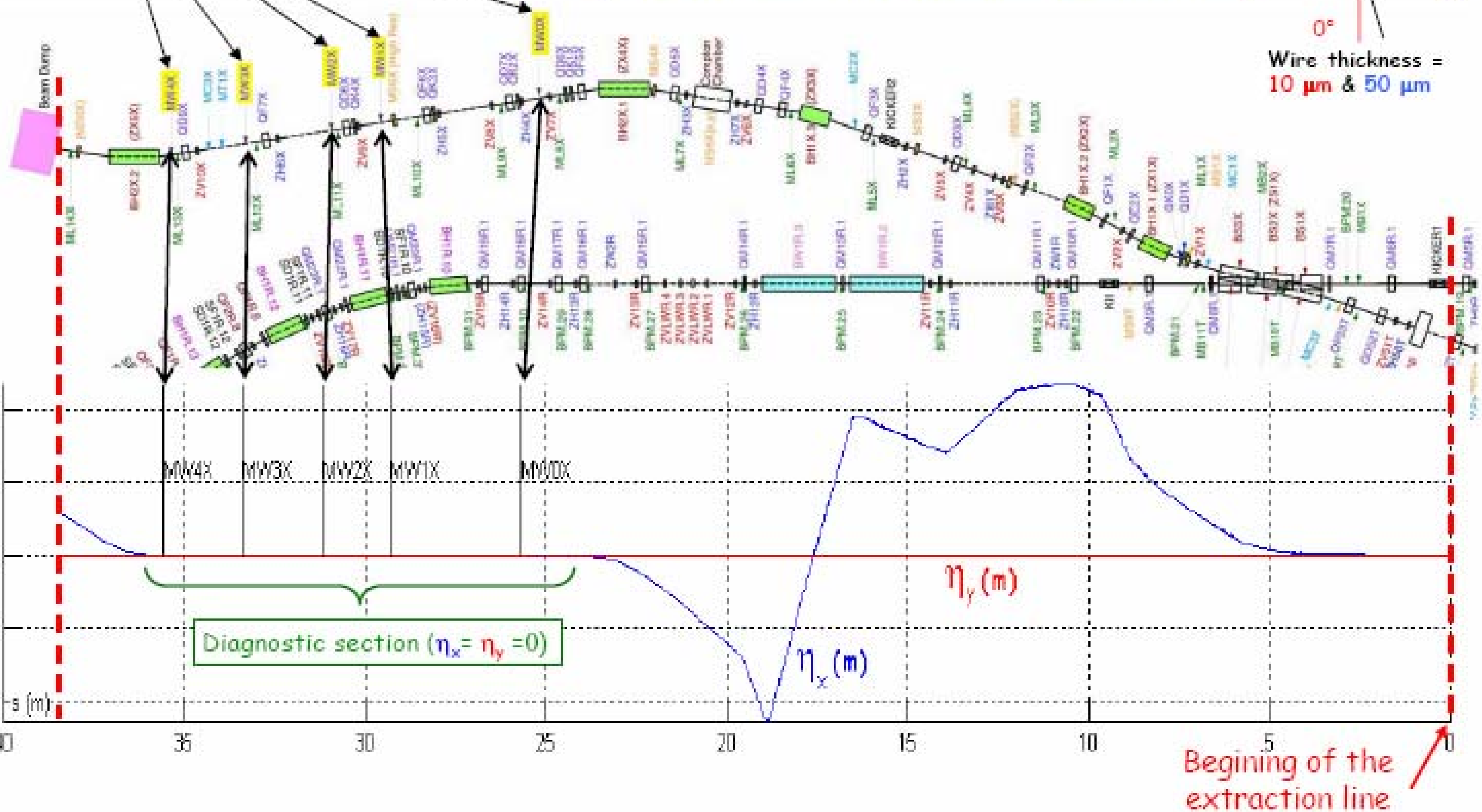

Vertical emittance growth in ATF Extraction Line

Measured vertical emittances are higher than expected, and there is a dependence with the beam current.

Vertical emittance in the DR
Vertical emittance in the EXT line

S. Kuroda et al.

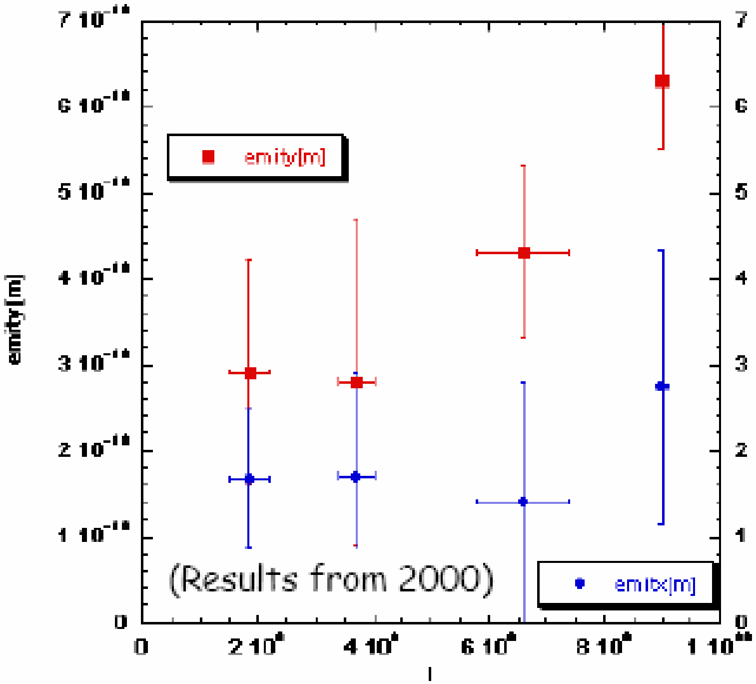

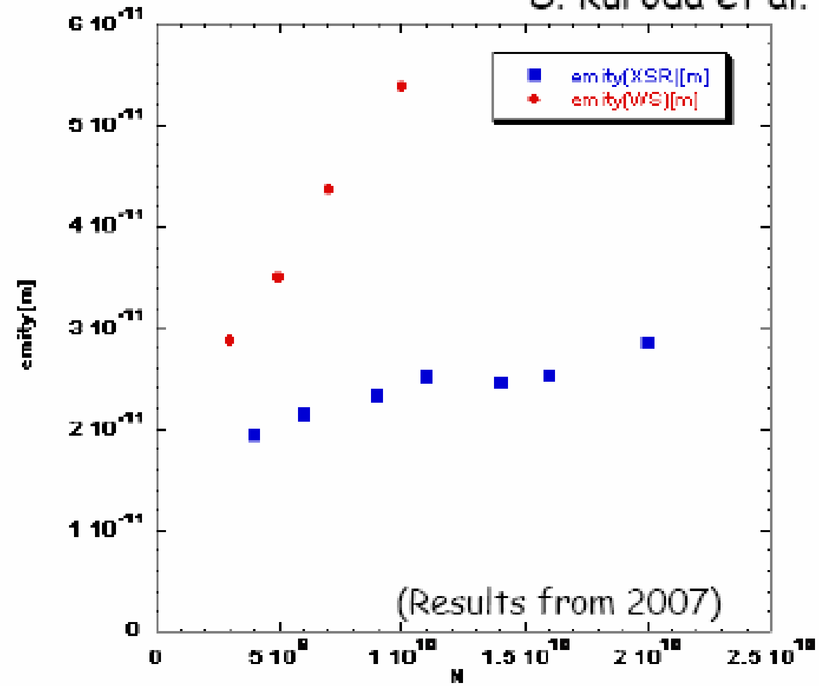

Hypotheses
- Non linearity → coupling
-Intensity dependence: wakefields, orbit (BPM) ?

→ Emittance measurement accuracy ?

2 - Multi-wire scanner emittance reconstruction method

No coupling between reference point and wire scanner position → the following linear system is used to reconstruct the vertical projected emittance.

$$\begin{pmatrix} \sigma_{33}^{MW0X} \\ \sigma_{33}^{MW1X} \\ \dots \\ \sigma_{33}^{MW4X} \end{pmatrix} = \begin{pmatrix} R_{33}^{(A->MW0X)2} & 2R_{33}^{(A->MW0X)}R_{34}^{(A->MW0X)} & R_{34}^{(A->MW0X)2} \\ R_{33}^{(A->MW1X)2} & 2R_{33}^{(A->MW1X)}R_{34}^{(A->MW1X)} & R_{34}^{(A->MW1X)2} \\ \dots & \dots & \dots \\ R_{33}^{(A->MW4X)2} & 2R_{33}^{(A->MW4X)}R_{34}^{(A->MW4X)} & R_{34}^{(A->MW4X)2} \end{pmatrix} \begin{pmatrix} \sigma_6^A \\ \sigma_9^A \\ \sigma_{10}^A \end{pmatrix} = M_Y \begin{pmatrix} \sigma_6^A \\ \sigma_9^A \\ \sigma_{10}^A \end{pmatrix}$$

$$\sigma_{33}^{MWiX} = \left(\sigma_y^{measure@MWiX}\right)^2 - \left(\frac{d_{y\_wire}}{4}\right)^2 - \left(\frac{\Delta p}{p} * \eta_y^{MWiX}\right)^2$$

at the 5 wire scanners station

R_{ij} Linear transport coefficent

Beam matrix element at the reference point « A ».

The y-beam size are corrected from wire scanner diameter d_{y_wire} and dispersion η_y (assuming $\Delta p/p = 8.10^{-4}$)

σ_x measurements to defined σ_1 σ_2 and σ_3

$\sigma_{10°}$ measurements to defined σ_4 σ_5 σ_7 and σ_8

$$\sigma^A = \begin{pmatrix} \sigma_1^A & \sigma_2^A & \sigma_4^A & \sigma_7^A \\ \sigma_2^A & \sigma_3^A & \sigma_5^A & \sigma_8^A \\ \sigma_4^A & \sigma_5^A & \sigma_6^A & \sigma_9^A \\ \sigma_7^A & \sigma_8^A & \sigma_9^A & \sigma_{10}^A \end{pmatrix}$$

The reference point « A » is just in front MW0X wire scanner.

We will **focused on projected ε_y emittance** (*the other components will be analysed later*).

The Least Means Square Method (LMS) is used to find « the LMS solution ».

Then the projected emittance ε_y is computed using :

$$\varepsilon_y = \sqrt{\sigma_6^A.\sigma_{10}^A - \left(\sigma_9^A\right)^2}$$

Emittance measurements using quadrupole and skew quadrupole scans

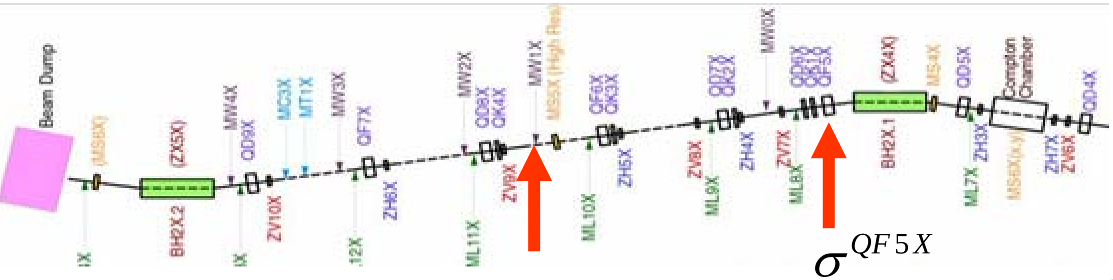

$$\sigma^{QF5X}$$

$$\sigma^{MW1X} = R\sigma^{QF5X}R^T$$

Transfer Matrix $R = SQ$ with

$$S = \begin{pmatrix} S_{11} & S_{12} & 0 & 0 \\ S_{21} & S_{22} & 0 & 0 \\ 0 & 0 & S_{33} & S_{34} \\ 0 & 0 & S_{43} & S_{44} \end{pmatrix} \quad Q = \begin{pmatrix} 1 & 0 & 0 & 0 \\ k & 1 & 0 & 0 \\ 0 & 0 & 1 & 0 \\ 0 & 0 & -k & 1 \end{pmatrix}$$

The measured beam sizes, σ^M, at MW1X are expressed as a parabolic function of the strength of QF5X, described by 3 fit parameters. Reconstructing those parameters make enable the twiss parameter determination at QF5X position, via the reconstruction of σ_{11}, σ_{12}, σ_{22}, σ_{33}, σ_{34}, σ_{44}.

$$\sigma_{11}^M = S_{11}^2\sigma_{11}^{QF} + 2S_{11}S_{12}\sigma_{12}^{QF} + S_{12}^2\sigma_{22}^{QF} + k(S_{11}\sigma_{11}^{QF} + S_{12}\sigma_{12}^{QF})2S_{12} + k^2\sigma_{11}^{QF}S_{12}^2 \Leftrightarrow A_x(k-B_x)^2 + C_x$$

$$\sigma_{33}^M = S_{33}^2\sigma_{33}^{QF} + 2S_{33}S_{34}\sigma_{34}^{QF} + S_{34}^2\sigma_{44}^{QF} + k(S_{33}\sigma_{33}^{QF} + S_{34}\sigma_{34}^{QF})2S_{34} + k^2\sigma_{33}^{QF}S_{34}^2 \Leftrightarrow A_y(k-B_y)^2 + C_y$$

$$\sigma_{11}^Q = \frac{A_x}{S_{12}^2}$$

$$\sigma_{22}^Q = \frac{1}{S_{12}^2}\left(A_xB_x^2 + 2\frac{S_{11}}{S_{12}}A_xB_x + \frac{S_{11}^2}{S_{12}^2}A_x + C_x\right)$$

$$\sigma_{12}^Q = -\frac{A_x}{S_{12}^2}\left(B_x + \frac{S_{11}}{S_{12}}\right)$$

$$\Rightarrow \varepsilon_x = \sqrt{\sigma_{11}^Q\sigma_{22}^Q - \sigma_{12}^Q} = \sqrt{\frac{A_xC_x}{S_{12}^4}}$$

And the same for $\sigma_{33}\,\sigma_{34}\,\sigma_{44} \rightarrow \varepsilon_y$

Emittance measurements using quadrupole and skew quadrupole scans

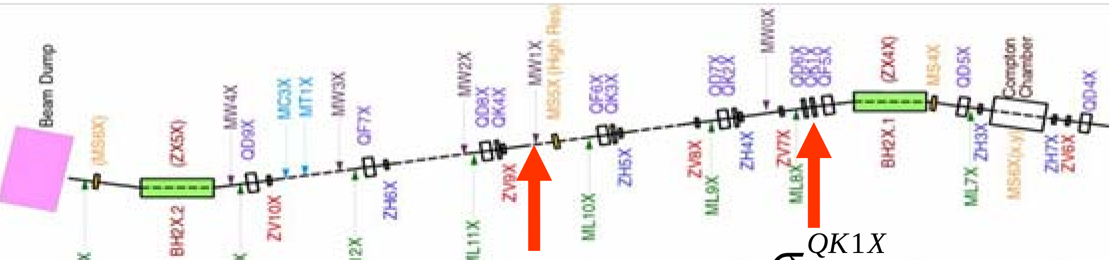

σ^{QK1X}

$$\sigma^{MW1X} = R\sigma^{QK1X}R^T$$

Transfer Matrix $R = SQ$ with

$$S = \begin{pmatrix} S_{11} & S_{12} & 0 & 0 \\ S_{21} & S_{22} & 0 & 0 \\ 0 & 0 & S_{33} & S_{34} \\ 0 & 0 & S_{43} & S_{44} \end{pmatrix} \quad Q = \begin{pmatrix} 1 & 0 & 0 & 0 \\ 0 & 1 & k & 0 \\ 0 & 0 & 1 & 0 \\ k & 0 & 0 & 1 \end{pmatrix}$$

The measured beam sizes, σ^M, at MW1X are expressed as a parabolic function of the strength of QK1X, described by 3 fit parameters. If no coupling, the parabola is centered at zero.

$$\sigma_{11}^M = S_{11}^2\sigma_{11}^{QK} + 2S_{11}S_{12}\sigma_{12}^{QK} + S_{12}^2\sigma_{22}^{QK} + k(S_{11}\sigma_{13}^{QK} + S_{12}\sigma_{23}^{QK})2S_{12} + k^2\sigma_{33}^{QK}S_{12}^2 \Leftrightarrow D_x(k - E_x)^2 + F_x$$

$$\sigma_{33}^M = S_{33}^2\sigma_{33}^{QK} + 2S_{33}S_{34}\sigma_{34}^{QK} + S_{34}^2\sigma_{44}^{QK} + k(S_{33}\sigma_{13}^{QK} + S_{34}\sigma_{14}^{QK})2S_{34} + k^2\sigma_{11}^{QK}S_{34}^2 \Leftrightarrow D_y(k - E_y)^2 + F_y$$

$$D_x = S_{12}^2\sigma_{33}^{QK} \qquad D_y = S_{34}^2\sigma_{11}^{QK}$$

$$-D_xE_x = S_{12}(S_{11}\sigma_{13}^{QK} + S_{12}\sigma_{23}^{QK}) \qquad -D_yE_y = S_{34}(S_{33}\sigma_{13}^{QK} + S_{34}\sigma_{14}^{QK})$$

$$D_xE_x^2 + F = S_{11}^2\sigma_{11}^{QK} + 2S_{11}S_{12}\sigma_{12}^{QK} + S_{12}^2\sigma_{22}^{QK} \qquad D_yE_y^2 + F = S_{33}^2\sigma_{33}^{QK} + 2S_{34}S_{33}\sigma_{34}^{QK} + S_{34}^2\sigma_{44}^{QK}$$

σ_{11}, σ_{12}, σ_{22}, σ_{33}, σ_{34}, σ_{44}.at QK1X can be deduced from previous step, knowing the R matrix (QF5X + drift). To determine coupling elements σ_{13}, σ_{23}, σ_{14} one needs measurements at 2 wires scanners.

Results from 12 march 2008 shift

The vertical emittance in the DR was measured :

ε_x = 5 nm.rad (?)

ε_y = 34 pm.rad

$$\sigma_y = \sqrt{\varepsilon_y \beta_y + (\eta_y \delta)^2}$$

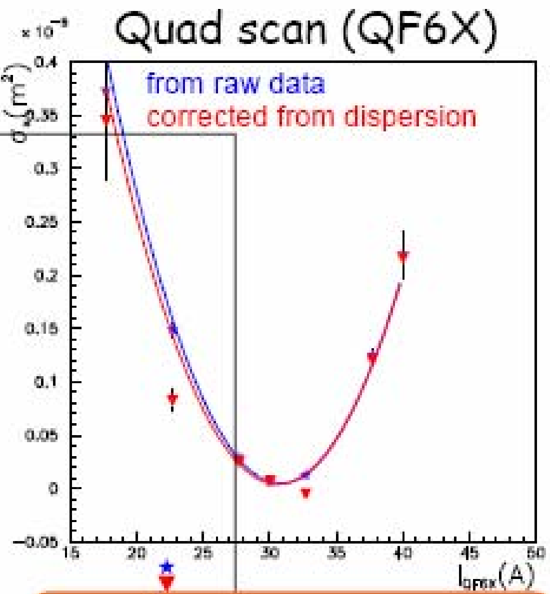

ε_x= (3.3 +/- 0.4) nm.rad

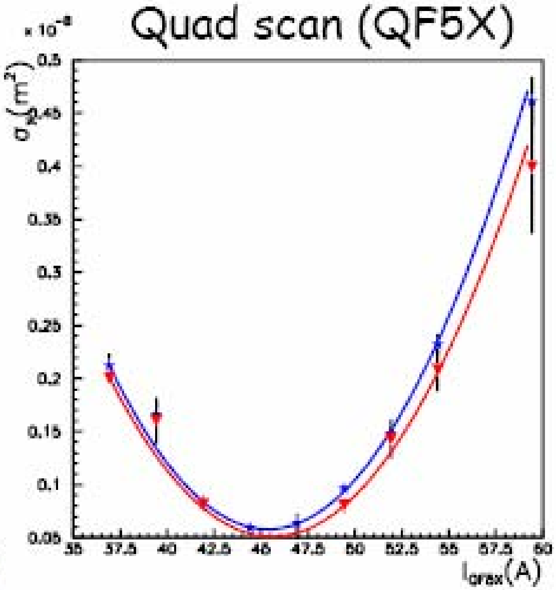

ε_y= (114 +/- 13) pm.rad

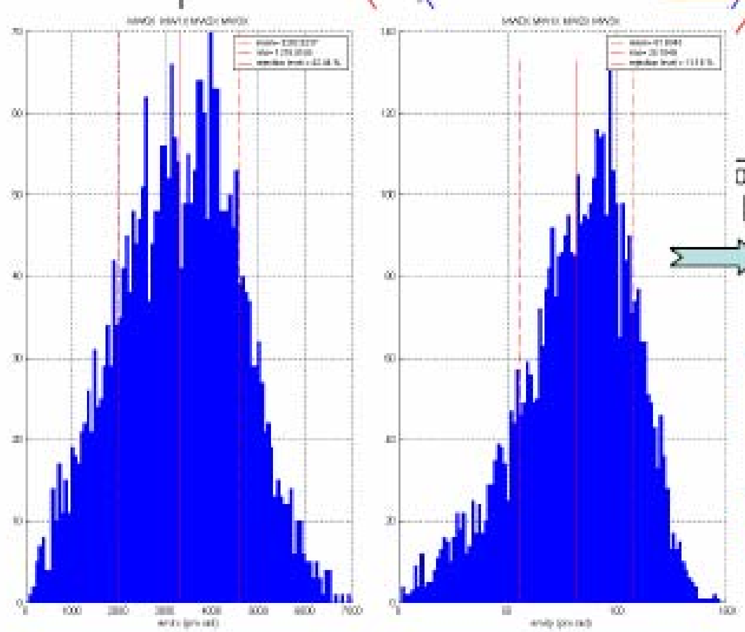

Multi-wire emittance reconstruction based on Monte-Carlo simulation :

ε_x= (3.3 +/- 1.3) nm.rad ~ 0.66% DR value (?)

ε_y= (82 +/- 26) pm.rad ~ 300 % DR value

Twiss parameters From QD8 scan

βy=41+/-9 m

αy=-10+/-3

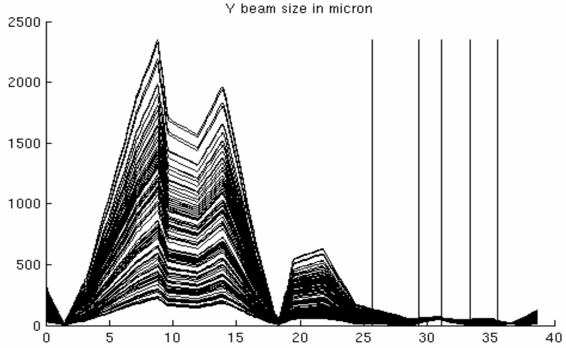

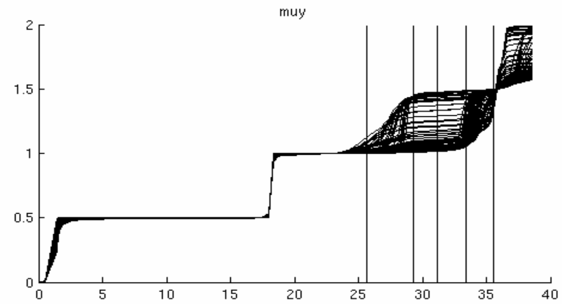

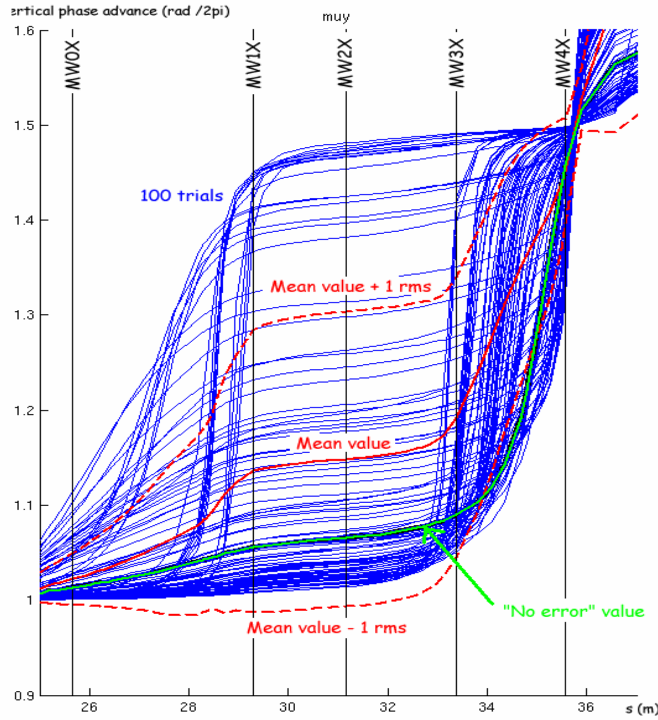

βy=41+/-3 m

αy=-10+/-1

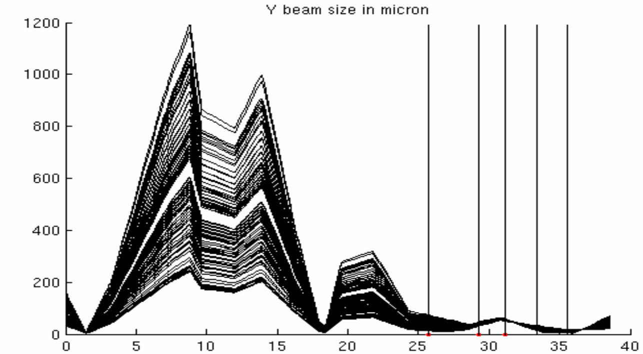

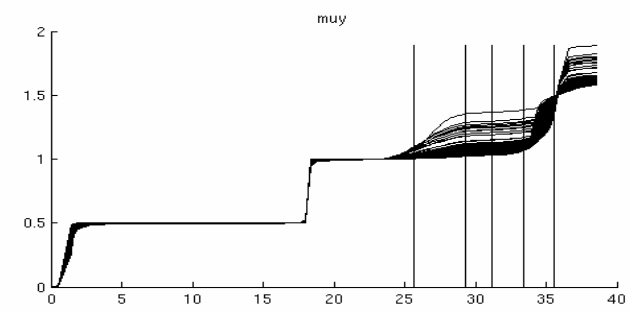

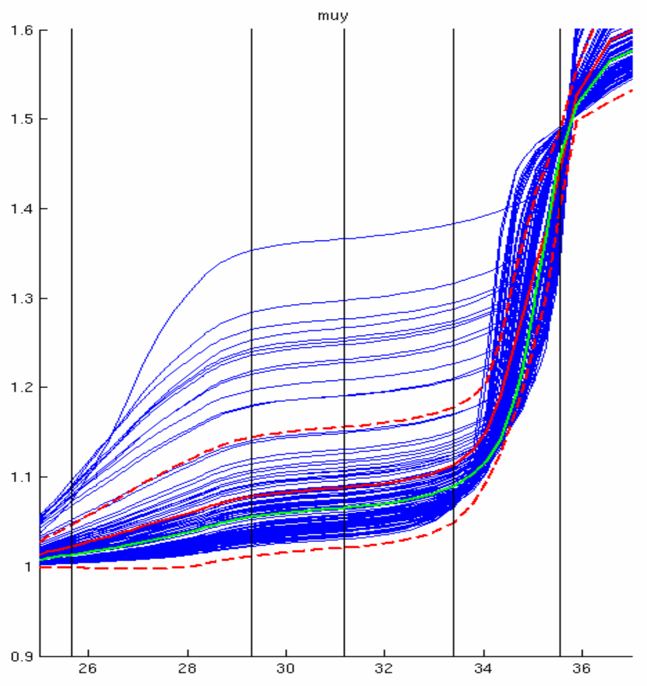

4.7-Search for uniqueness of coupling mimics

With Skew set at QM7 @3A (0.01547m-1)and vertical emittance @51 pm.rad.

With Skew set at BS3X @1.8A (0.00928m-1) and vertical emittance @51 pm.rad.

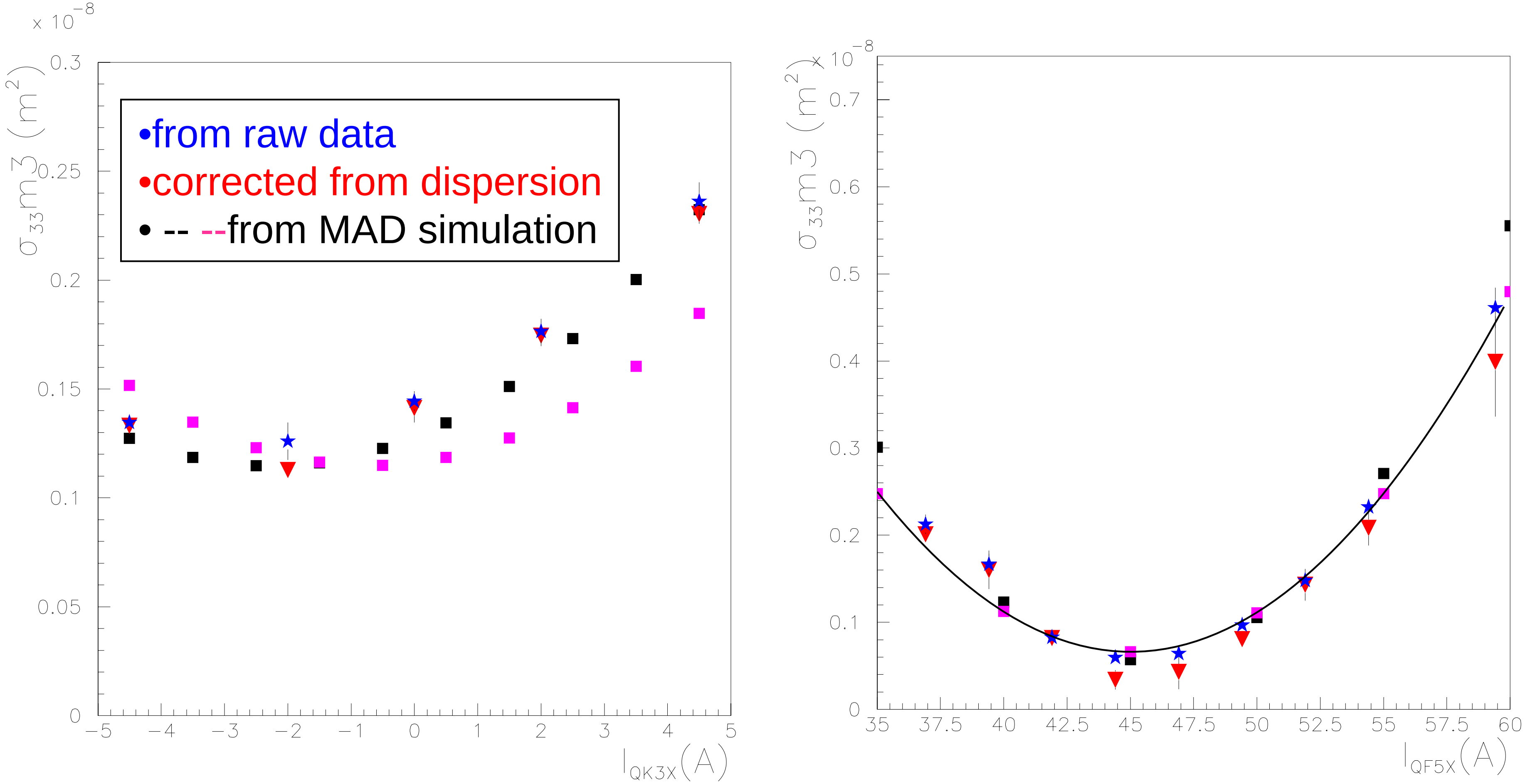

Problem: can't achieve to reproduce measurement with MAD simulation

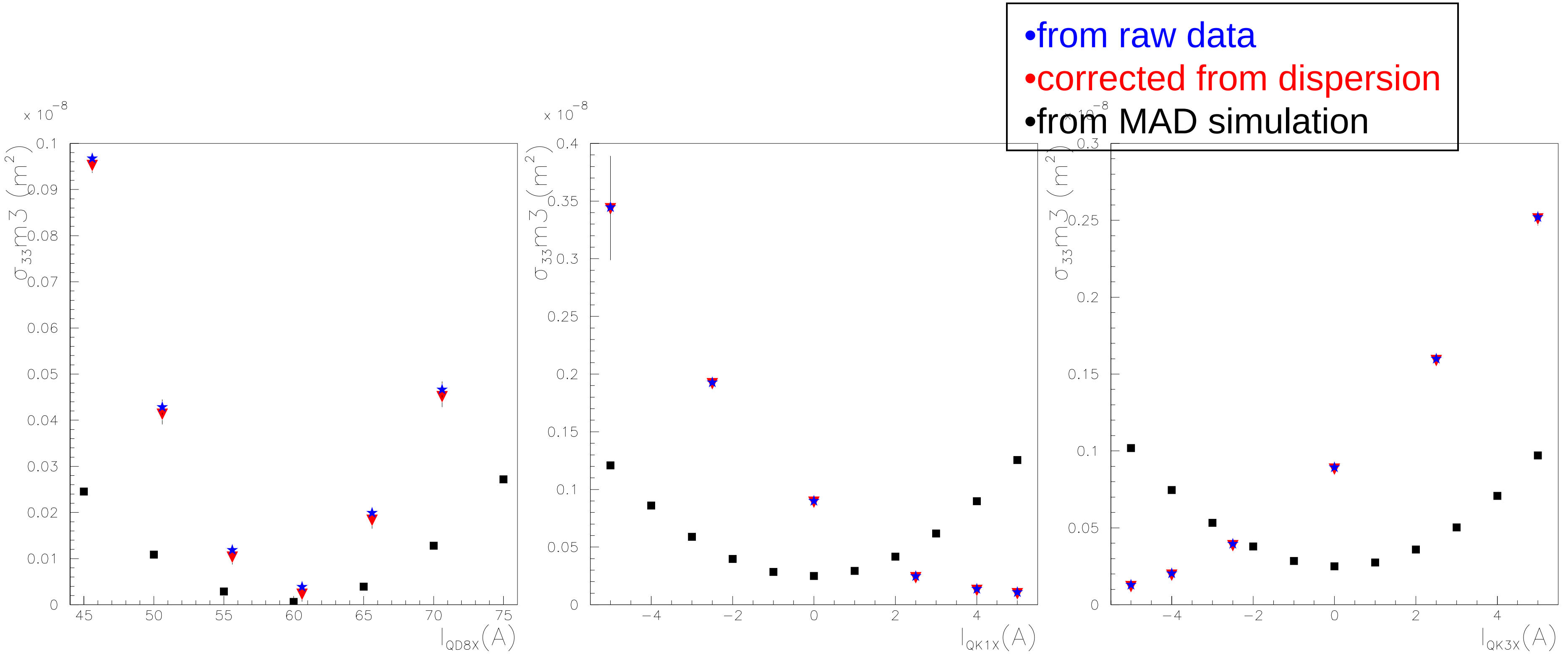

Skew quad scans show coupling. Try to reproduce all quad measurements with MAD introducing sources of coupling in ExtLine. For the moment, a unique source at QM7 can not explain what we observe. Still under investigation....

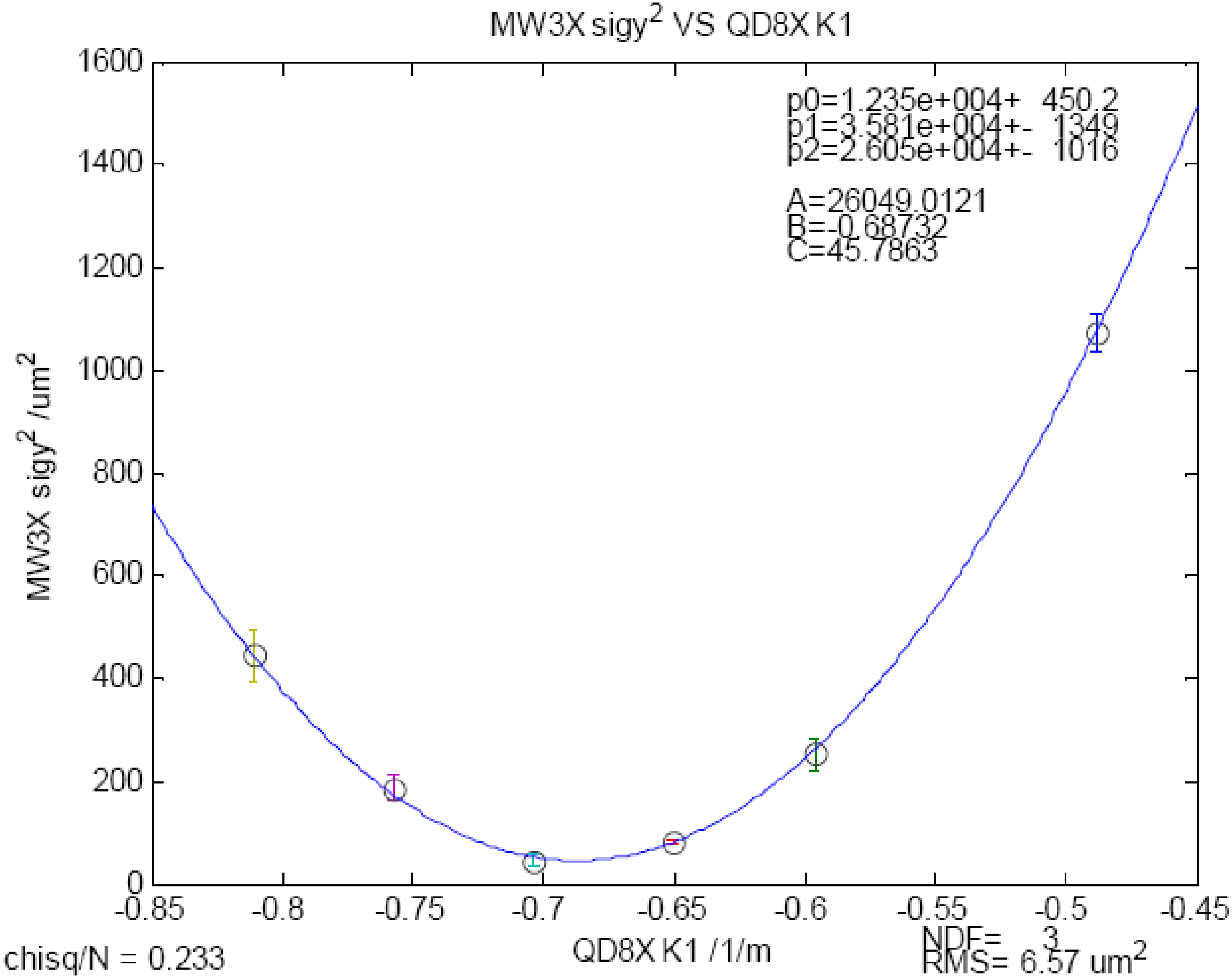
MW3X sigy^2 VS QD8X K1
p0=1.235e+004+ 450.2
p1=3.581e+004+- 1349
p2=2.605e+004+- 1016
A=26049.0121
B=-0.68732
C=45.7863
MW3X sigy^2 /um^2
QD8X K1 /1/m
1600
1400
1200
1000
800
600
400
200
0
-0.85
-0.8
-0.75
-0.7
-0.65
-0.6
-0.55
-0.5
-0.45
chisq/N = 0.233
NDF= 3
RMS= 6.57 um^2

Extraction line vertical emittance growth ?

→ Could magnets shared with damping ring be the cause of the effect ?

Shared magnets with the Damping Ring

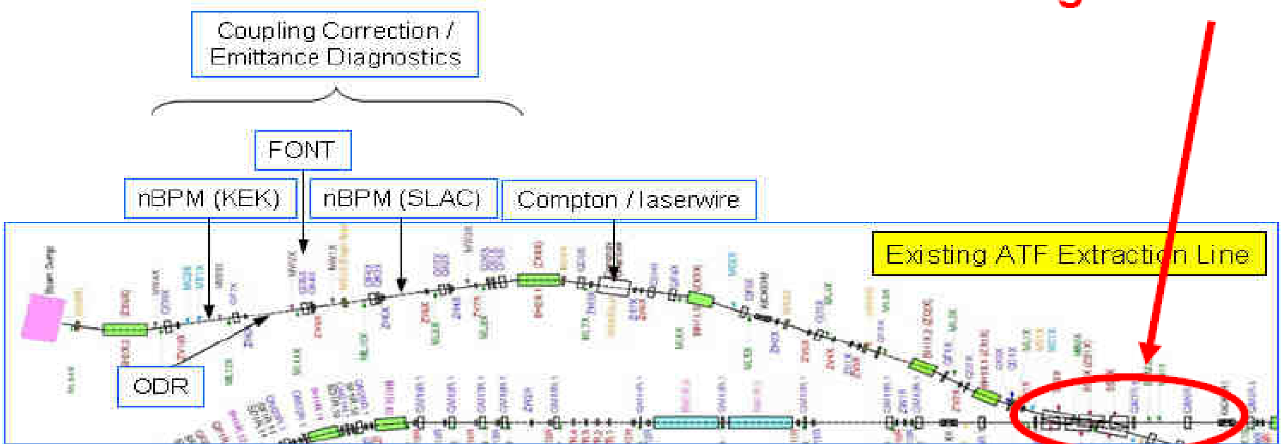

Septum magnets + Q7 and Q6 quadrupoles

The extracted beam passes off-axis

Non-linearities of the field

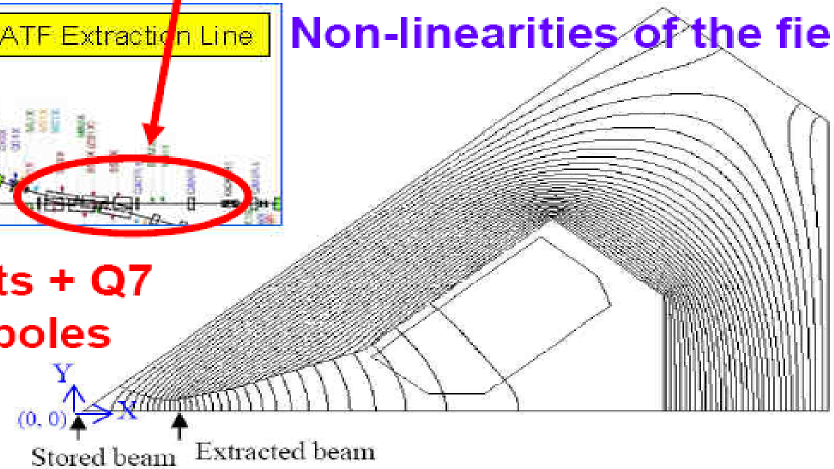

x= 2.2 cm

Vertical emittance in the DR
Vertical emittance in the EXT line

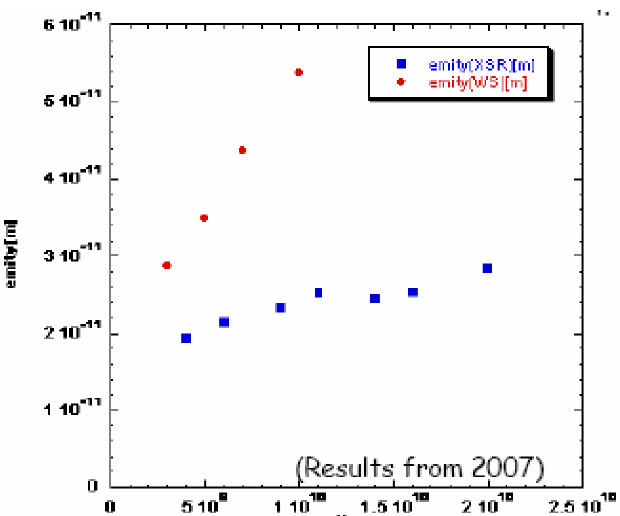

→ Seems only partial explanation, even at low intensities…

Emittance growth studies using static bumps in the ATF EXT line

Tracking simulations in the Extraction Line

- With bumps created with ZV9R and ZV100R
- Including non-linearity in QM7
- For different input emittances

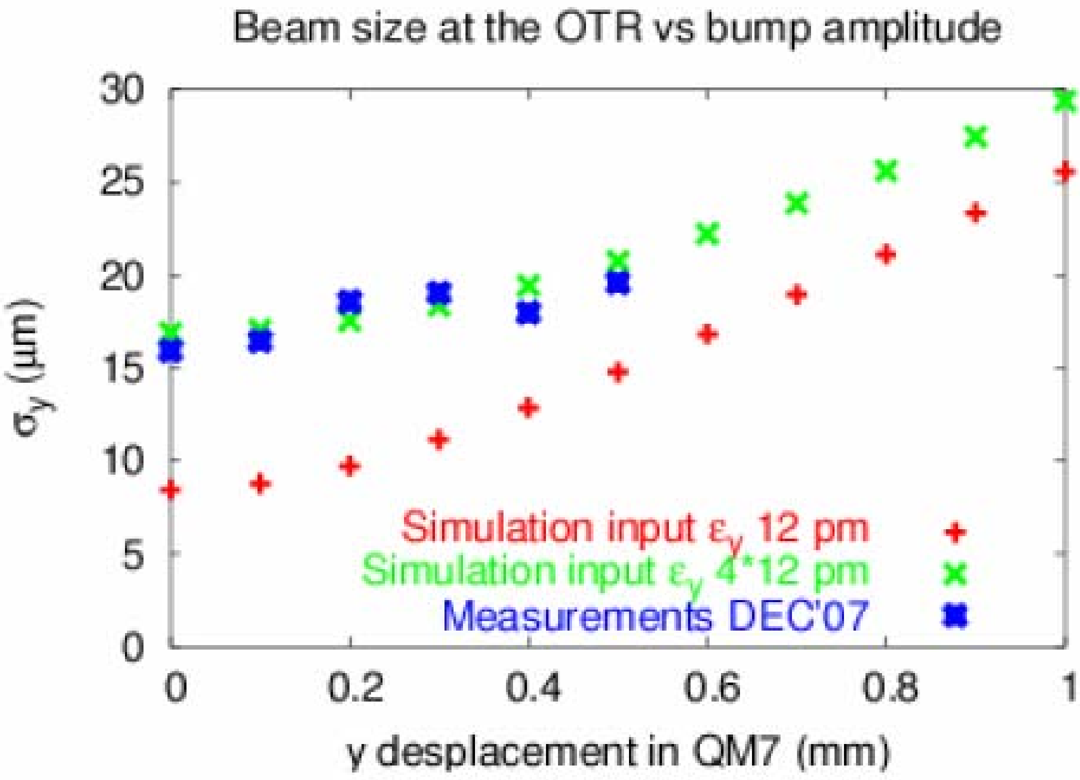

Considering 0.5 mm bump:

- with nominal input emittances, beam size increase in OTR is a factor ~1.8

-with ε_y 4 times nominal, beam size increase in OTR is a factor ~1.2 as in the measurements

QM7 2D field calculation with PRIAM

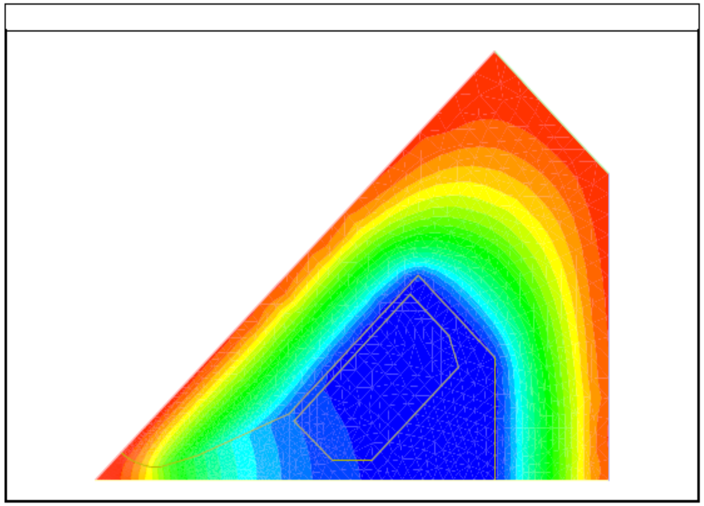

FIG. 5 – QM7 B field lines

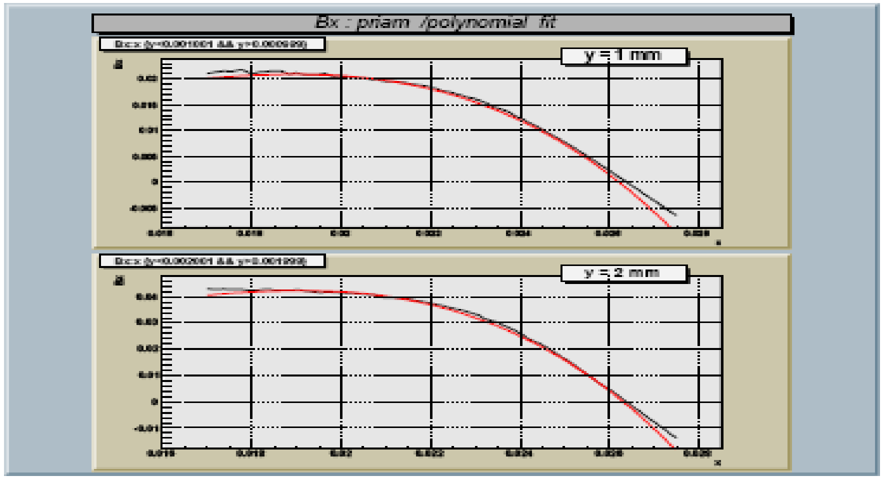

FIG. 6 – QM7 Bx at y cst

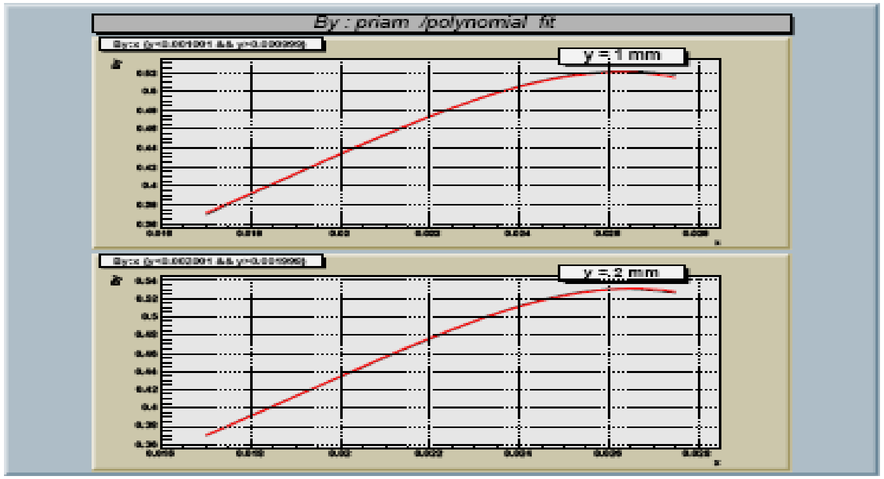

FIG. 7 – QM7 By at y cst

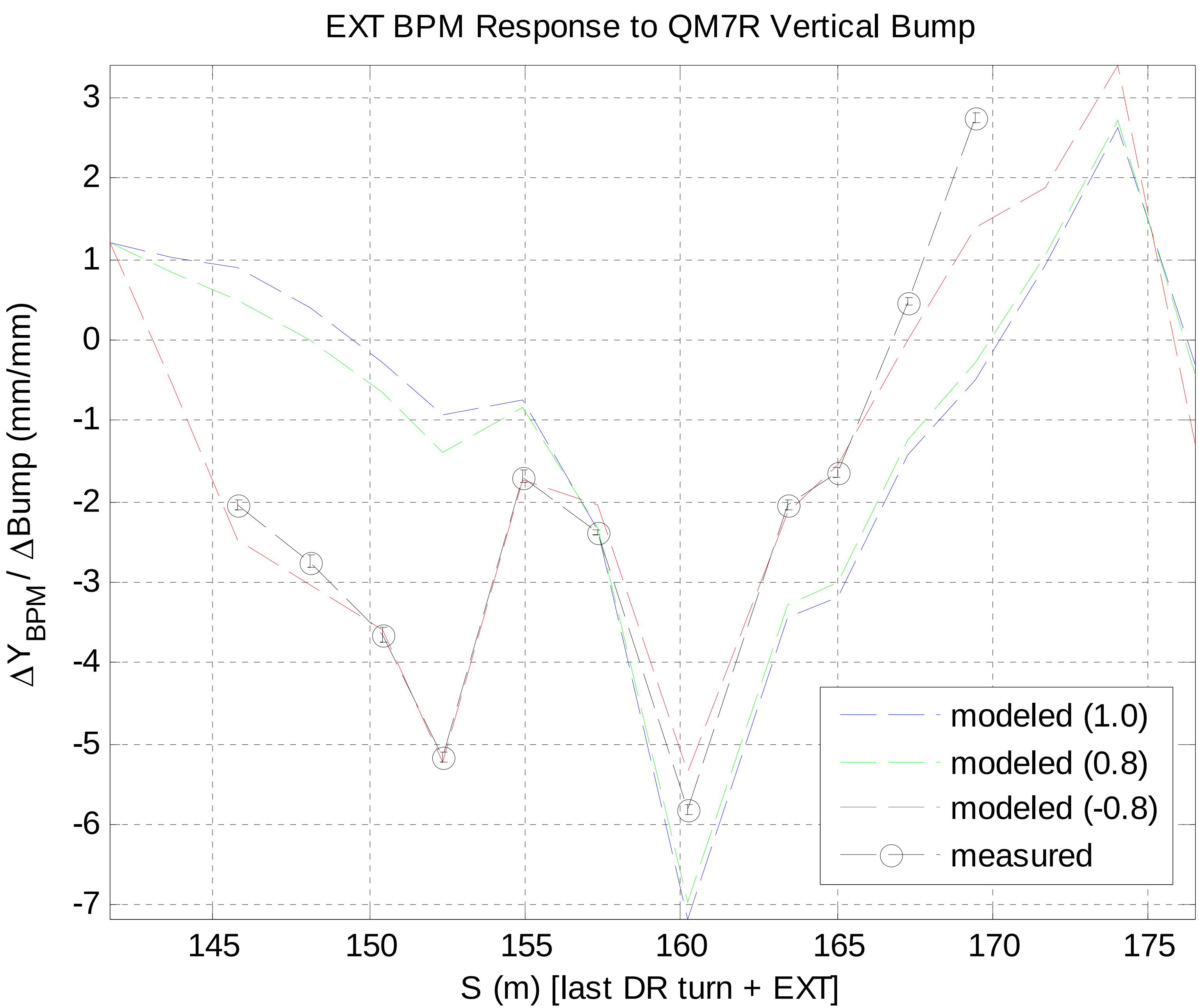

EXT BPM Response to QM7R Vertical Bump
ΔY_BPM / ΔBump (mm/mm)
S (m) [last DR turn + EXT]
3
2
1
0
-1
-2
-3
-4
-5
-6
-7
145
150
155
160
165
170
175
modeled (1.0)
modeled (0.8)
modeled (-0.8)
measured

Conclusions and prospects

- ATF EXT projected vertical emittance consistently measured ~ 3 times DR values at 5 10^{10} e^-/bunch
- Quad scans more precise than multi-wire technique to measure projected X and Y emittances & Twiss parameters, due to small betatron phase separation between wire scanners in present EXT line – the latter should improve in new ATF2 EXT line thanks to better optical design.
- Identified reason for vertical projected emittance growth : QM7 DR quad, traversed off-axis by EXT beam, can induce x-y coupling through the sextupole field component in the presence of a vertical offset. However modeling and beam size measurements at downstream OTR suggests it cannot be sole explanation. Spurious η_y at OTR leaking out from DR must also be controlled not to mask effects.
- Full 4D beam matrix measurements required to determine linear coupling source(s) & correction. Set of normal and skew quad scans are investigated, combining X, Y and 10° wire measurements
→ may be more precise & reliable than traditional multi-wire 4D technique in which <xy> determination suffers from unfavorable error propagation.
- Significant phase-space variations are found at EXT input on successive shifts :
→ time-consuming pre-tuning needed before any sensible investigations in EXT line are performed,
→ need to optimize shift planning in this respect + work on reproducibility of DR optical tuning.
- Reliable control of apparent vertical emittance growth from x-y coupling in ATF2 EXT line will require precise Twiss parameter, dispersion & trajectory control on time-scale of typically 1 shift, in addition to x-y coupling correction ability further downstream.
- Automation of procedures essential for speed & reliability → develop all tools in “Flight Simulator”.
- More efficient collaborative multi-partner / site team work → better defined procedures and information flow during and after shifts, with improved sharing of data & algorithms : check-lists and measurement programs, common data areas, on-call experts for specialist topics & questions, standardized scheme to upload e-log book & shift reports, respectively during and after shifts.
- Dedicated instrumentation → investigate adding 2D profile measurements based on OTR stations near each wire-scanners in ATF2 EXT line, for multiple & fast <xx>, <yy> and <xy> measurements.